Langmuir

Letter

pubs.acs.org/Langmuir

Shrink-Induced Silica Multiscale Structures for Enhanced Fluorescence from DNA Microarrays

Himanshu Sharma,[†,∥] Jennifer B. Wood,[‡,∥] Sophia Lin,[†] Robert M. Corn,[‡,§] and Michelle Khine*[,†,§]

[†]Department of Chemical Engineering & Materials Science, [‡]Department of Chemistry, and [§]Department of Biomedical Engineering, University of California, Irvine, Irvine, California 92697, United States

Supporting Information

ABSTRACT: We describe a manufacturable and scalable method for fabrication of multiscale wrinkled silica (SiO_2) structures on shrink-wrap film to enhance fluorescence signals in DNA fluorescence microarrays. We are able to enhance the fluorescence signal of hybridized DNA by more than 120 fold relative to a planar glass slide. Notably, our substrate has improved detection sensitivity (280 pM) relative to planar glass slide (11 nM). Furthermore, this is accompanied by a 30−45 times improvement in the signal-to-noise ratio (SNR). Unlike metal enhanced fluorescence (MEF) based enhancements, this is a far-field and uniform effect based on surface concentration and photophysical effects from the nano- to microscale SiO_2 structures. Notably, the photophysical effects contribute an almost 2.5 fold enhancement over the concentration effects alone. Therefore, this simple and robust method offers an efficient technique to enhance the detection capabilities of fluorescence based DNA microarrays.

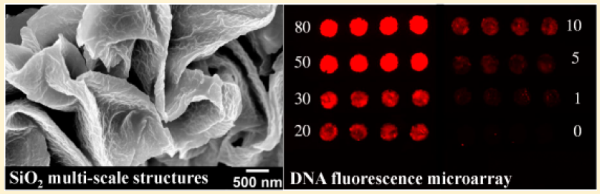

INTRODUCTION

The development of DNA microarrays has proven invaluable for high throughput quantification of gene expression profiling, genomic analysis, disease diagnosis, and drug screening.[1−3] Fluorescence-based DNA microarrays offer numerous advantages, such as high sensitivity and multiplexing capabilities.[4,5] Despite these benefits, the challenge to improve the detection sensitivity persists.[6,7] Strategies to increase the fluorescence sensitivity of DNA microarrays include increasing the amount of the capture probes or alternatively, amplifying the fluorescence signal using surface enhancements. To increase the density of DNA probes immobilized on the surface, techniques involving nanostructured substrates using three-dimensional structures, such as dendrimeric/nanopillar-like structures or grafting polyethylene glycol (PEG) layers onto silanized glass slides, have been pursued.[7−12] Increases in the fluorescence intensity of 2−30-fold were observed using these approaches to enhance the DNA probe density. However, oversaturation of probe density can reduce target DNA binding efficiency because of strong electrostatic repulsions, which leads to retardation of hybridization kinetics.[8,13] To enhance the observed fluorescence signal, noble metal nanostructures and nanoparticles have also served as attractive approaches. These techniques use surface plasmons to modify and improve the spectral and photophysical properties of fluorophores.[14,15] However, these metallic structures typically require precise and sophisticated equipment to yield near-field metal enhanced fluorescence (MEF) effects (within nanometric lengths from the surface) in heterogeneous areas of "hot spots".[16,17]

Reflective surfaces such as silica (SiO_2) on silicon (Si) have also been employed as a platform for enhancing fluorescence microarrays.[18,19] These reflective substrates typically require a transparent spacer layer provided by the SiO_2 between the reflective surface (Si) and the fluorescent material. The fluorescence signal enhancement is based on the principle of optical interference.[20] In addition to their optical properties, SiO_2 surfaces have also been attractive surfaces for their high biocompatibility properties and the ease of surface functionalization.[21] Similarly, it has been reported that encapsulation of dyes into SiO_2-based nanoparticles can also enhance the fluorescence signal.[22] In particular, the use of dye-doped SiO_2 nanoparticles has presented significant interest due to its advantageous high surface-to-volume ratio, photochemical stability, and ability to amplify the fluorescent signal.[23] The mechanism of fluorescence enhancements is related to the internal SiO_2 architectures shielding the fluorescent dyes from being quenched by its surroundings, thus reducing the kinetics of the irradiative decay of the excited fluorophores.[22,23] Furthermore, immobilization of the fluorescent dye within the SiO_2 matrix has been thought to restrict the mobility and flexibility of the molecules, which can lead to reduced nonradiative relaxation and subsequently increased photoemission brightness.[23−25]

However, typical enhancements from this approach have been modest, with increases in the fluorescence signal of 5−30 fold.[8] Recently, Lin et al. reported generating SiO_2 structures from a precoated thermoplastic polyolefin (PO) shrink film (PO-SiO_2) to enhance the fluorescence signal of bound biotin−streptavidin−tetramethylrhodamine isothiocyanate (TRITC) biomolecules.[26] In this Letter, we expand upon this strategy

Received: March 24, 2014
Revised: August 8, 2014
Published: September 5, 2014

   dx.doi.org/10.1021/la501123b | *Langmuir* 2014, 30, 10979−10983

and demonstrate its applicability to DNA fluorescence microarrays. We improve the limit of detection (LOD) sensitivity of the DNA hybridization assay by more than 40-fold compared to controls (a glass substrate). Our results demonstrate that our PO-SiO_2 structured substrate is an attractive approach for DNA fluorescence microarrays.

EXPERIMENTAL SECTION

The fabrication of these substrates is simple, inexpensive, robust, and scalable. To prepare the substrate, a laser cut tape mask composed of a four by eight array of 1 mm in diameter holes with center to center spacing of 1.9 mm was applied to a clean PO shrink film (955-D, Sealed Air Corporation, 1 mil) prior to sputter deposition of 20 nm SiO_2 to generate PO-SiO_2 substrate (Figure 1a,b). The PO-SiO_2 substrate was chemically

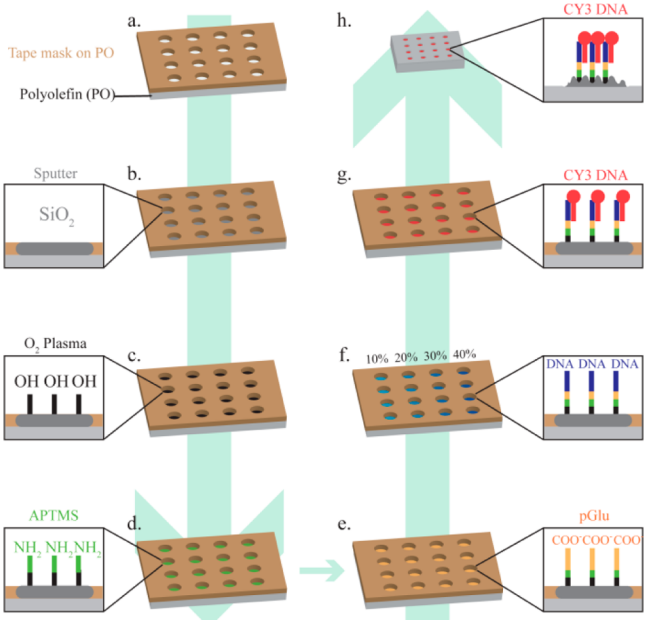

Figure 1. Schematic for fabrication of DNA fluorescence microarray on shrunk PO-SiO_2.

activated by oxygen (O_2) plasma treatment and immersed into a solution of 3-(aminopropyl) trimethoxysilane (APTMS) in ethanol (2% v/v) for 45 min at room temperature (Figure 1c,d). The substrates were rinsed with ethanol and cured overnight in ambient conditions. For DNA probe attachment, primary amine groups were covalently linked to the amine-functionalized PO-SiO_2 substrates. To accomplish this, the PO-SiO_2 surfaces were incubated with 2 mg/mL poly-L-glutamic acid (pGlu) in phosphate buffered saline (PBS) buffer for 1 h (Figure 1e). The pGlu binds to the amine-functionalized PO-SiO_2 surface through electrostatic interactions. 250 μM amine-modified single stranded (A_{30} ssDNA) solution in a PBS buffer that contained 75 mM 1-ethyl-3-(3-(dimethylamino)propyl)-carbodiimide hydrochloride (EDC) and 15 mM *N*-hydroxysulfosuccinimide (NHSS) was prepared. Five-tenths of a microliter of two amine-terminated 30mer oligonucleotides A (A_{30} sequence: 5′-$NH_2(CH_2)_{12}(C_2H_6O_2)_{12}$AAAAAAAAAAAAAAAAAAAAAAAAAAAAAA-3′) and B (GFP sequence: 5′-$NH_2(CH_2)(C_2H_6O_2)_{12}$GATCTCGATCCCGCGAAATTAATAC-3′) with an A:B percentage of 80:20, 60:40, 50:50, 40:60, 30:70, 20:80, 10:90, 5:95, 1:99, 0.5:99.5, and 0:100 were incubated overnight on the PO-SiO_2 surfaces (Figure 1f). The initial stock concentration of the A_{30} sequence was always 250 μM, and the final concentration of the oligonucleotides in the mixture (A and B) was always 250 μM. After rinsing the PO-SiO_2 substrates with PBS and water, 0.5 μL of 1 μM complementary ssDNA to A_{30} tagged with Cy3 fluorophore was allowed to react for 40 min at room temperature, 22 °C (Figure 1g). After rinsing again with PBS and water, the substrates were dried with nitrogen (N_2), and then immediately imaged with an Olympus upright fluorescence microscope through a 2X microscope objective (Edmund Optics, NA = 0.055) and using a TRITC filter. The fluorescence intensities were analyzed using the region of interest (ROI) feature in ImageJ (National Institute of Health (NIH)). For each A:B percentage, we measured the fluorescence intensities from 16 spots and repeated this three independent times. PO-SiO_2 substrates were heated at around 160 °C for 2 min, which induced retraction of the PO shrink film (Figure 1h). This caused the thinner SiO_2 film to buckle and fold into nano- to microscale structures with high aspect ratios (Figure 2a,b). This

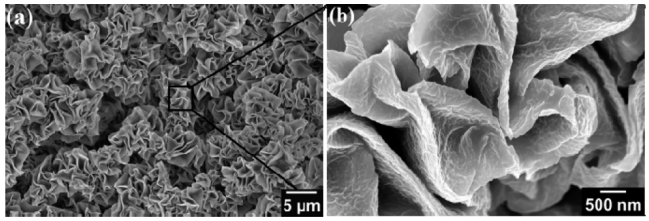

Figure 2. (a) Top-down SEM image of the shrunk PO-SiO_2 is a representative image of the heterogeneous populations of nano and microscale structures observed. (b) Zoomed in SEM image illustrating the micro and nanoscale features.

resulted in a PO-SiO_2 structured substrate referred to here on as shrunk PO-SiO_2. The substrates were imaged again with the Olympus upright fluorescence microscope at the same conditions as previously mentioned.

RESULTS AND DISCUSSION

Comparing the fluorescence images for the DNA microarray on the glass slide and shrunk PO-SiO_2 substrate, respectively, the dramatic fluorescence enhancements due to the substrate is apparent. As depicted in Figure 3a, the fluorescence signal at 80 and 50% A_{30} ssDNA on the shrunk PO-SiO_2 substrate was detectable while the fluorescence signals on the glass substrate at those concentrations were not discernible. In fact, even at the lowest concentration of 1% A_{30} ssDNA, the fluorescence signal could still be observed on the shrunk PO-SiO_2 substrate. Another noticeable difference is that, within the field of view selected (5 × 4 mm), 32 spots were visible on the shrunk PO-SiO_2 substrate, while three spots were visible on the glass slide. The image in Figure 3a has been stitched together to show more spots on the glass slide. This highlights the ability to rapidly detect multiple concentrations on the shrunk PO-SiO_2 substrate relative to a planar surface in regards to multiplexing capabilities. The dotted vertical white line represents where the plot profile was obtained for the different % of A_{30} ssDNA. The line profile shown in Figure 3b quantifies fluorescence signal uniformity over the SiO_2 islands on the shrunk PO-SiO_2 and glass slide substrates. Furthermore, the enhanced fluorescence signal observed on the shrunk PO-SiO_2 substrates is not localized to nanoscale regions, as with plasmonic effects. The larger working range on the PO-SiO_2 substrate is apparent by

dx.doi.org/10.1021/la501123b | *Langmuir* 2014, 30, 10979−10983

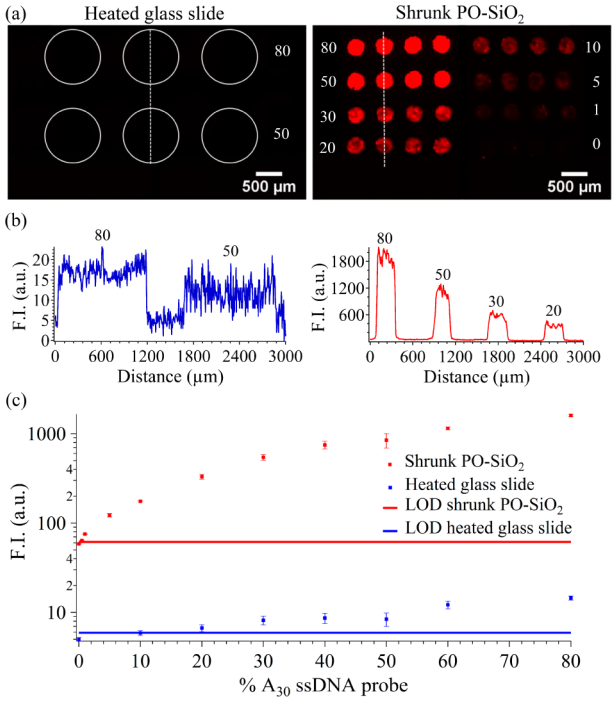

Figure 3. DNA fluorescence microarray of Cy3-DNA on heated glass slide and shrunk PO-SiO_2. (a) Fluorescence images of Cy3-DNA on heated glass and shrunk PO-SiO_2 and (b) their corresponding line plot profiles. (c) Average DNA fluorescence microarray intensities on heated glass and shrunk PO-SiO_2. F.I. corresponds to fluorescence intensity and the error bars are standard error of mean. The % single-stranded (s.s) DNA probe fluorescence images on the heated glass slide in panel (a) were stitched together for illustrative purposes and are not representative of the mask dimensions.

the average fluorescence intensities for each substrate (Figure 3c). The linear range on the shrunk PO-SiO_2 substrate was observed to be from 5−40% A_{30} ssDNA while on the glass slide, was observed to be from 10−30% A_{30} ssDNA. The detection limit (χ_{LOD}) was calculated, as shown in eq 1, by taking three times the standard deviation of the background signal, $\bar{\sigma}_{bg}$, on glass or the shrunk PO-SiO_2 substrate and adding the mean background signal, $\bar{\chi}_{bg}$.[27] The $\bar{\chi}_{bg}$ was measured by calculating the fluorescence intensity of the nonspecific binding of the Cy3 DNA to the 0:100% A_{30}:GFP ssDNA sequence on glass and shrunk PO-SiO_2.

$$\chi_{LOD} = \bar{\chi}_{bg} + 3\bar{\sigma}_{bg} \quad (1)$$

The concentration curve demonstrates that a relative surface coverage of 0.5% A_{30} ssDNA can be detected on the shrunk PO-SiO_2 substrate in contrast to about 20% A_{30} ssDNA observed on the glass slide. The results for the nonshrunk PO-SiO_2 surfaces are presented in Supporting Information Figure S1.

We also examined the performance of the DNA microarray in in the absence of EDC/NHS and in the absence both of EDC/NHS and pGlu. These results (Figure S2−S3) indicate that binding of A_{30} ssDNA was most successful in the presence of both EDC/NHS and pGlu. Fluorescence signal enhancement was measured quantitatively, and results were compared to that obtained from the DNA hybridized on the glass slide. The average fluorescence signal (FS) increase of the substrates is calculated according to eq 2, as previously reported, by measuring the mean FS obtained after heating (AH) ($\bar{\chi}_{ahs}$) minus the mean background FS AH ($\bar{\chi}_{ahbg}$) over the mean FS before heating (BH) ($\bar{\chi}_{bhs}$) minus the background FS BH ($\bar{\chi}_{bhbg}$).

$$FS_{avg} = \frac{\bar{\chi}_{ahs} - \bar{\chi}_{ahbg}}{\bar{\chi}_{bhs} - \bar{\chi}_{bhbg}} \quad (2)$$

As previously mentioned, the PO film shrinks by 77% in each length post heating, which leads to an approximately 20-fold concentration of surface area.[26] Lin et al. showed that with the substrate alone, a 14-fold increase in the fluorescence signal of TRITC was noted to occur with the biotin−streptavidin model system relative to the planar PO substrate and a 50-fold increase with the silica structures relative to the planar PO-SiO_2 substrate.[26] This increase in enhancement was determined to be due to photophysical effects of the highly scattering PO-SiO_2 structures. Here, the fluorescence signal of the Cy3-DNA was observed to increase by 45 times (standard error (S.E.) 3.5) on the shrunk PO-SiO_2 substrates relative to the planar PO-SiO_2 substrate. This is more than 2.5 times higher than expected due to concentrating alone. The integrated intensity of the entire DNA spots was calculated before and after shrinking on the PO-SiO_2 substrate for confirmation. A concentrating effect alone would result in the same integrated intensity value. Therefore, this additional increase in intensity is attributed to the optical effects.

Interestingly, more than a 120 fold (S.E. 5.00) increase in the fluorescence signal was observed on the shrunk PO-SiO_2 substrates relative to glass for 80−10% A_{30} ssDNA presented in Figure 4a. Furthermore, heating the hybridized DNA did not appear to significantly decrease the fluorescence signal. The

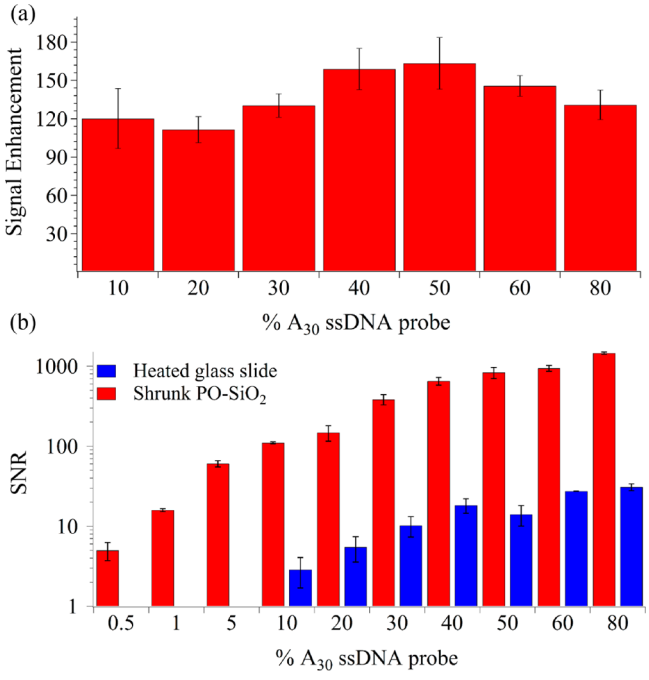

Figure 4. Analytical assessment of the improvement for different percentages of A_{30} ssDNA hybridized on the shrunk PO-SiO_2 substrate relative to the glass slide (a) A plot of the fluorescence signal increase on shrunk PO-SiO_2 substrate relative to heated glass (b) SNR on heated glass slide and shrunk PO-SiO_2 substrate for the hybridized DNA at various A_{30} ssDNA percentages. The error bars are standard error of mean.

dx.doi.org/10.1021/la501123b | Langmuir 2014, 30, 10979−10983

fluorescence signal was observed to decrease by less than 15% (S.E. 2.5%) over the different percentages of A_{30} ssDNA when comparing the hybridization signal on the heated glass slides to the signal prior to heating.

An increase in the fluorescence intensity was also coupled with a significant improvement in the signal-to-noise ratio (SNR) which is defined as the ratio of the average fluorescence signal minus the mean background signal to the standard deviation of the background, $\bar{\sigma}_{bg}$, as presented in eq 3.[28]

$$\mathrm{SNR} = \frac{\bar{X}_{ahs} - \bar{X}_{bg}}{\bar{\sigma}_{bg}} \quad (3)$$

For the SNR, any value higher than 3 is generally considered to be detectable.[29] The SNR shown in Figure 4b was noted to increase by more than 46-fold on the shrunk PO-SiO_2, 1455 (S.E. 35) for 80% A_{30} ssDNA relative to the glass slide, 30.87 (S.E. 0.15). For the glass slide, the limit in the SNR was 20% A_{30} ssDNA, while on the shrunk PO-SiO_2 substrate it was 0.5%. The limit in the SNR results supported the LOD results.

The enhancement in the fluorescence signal also resulted in an improvement in the detection sensitivity of the DNA microarrays. To assess the analytical detection performance of the shrunk PO-SiO_2 and glass substrates, the concentration corresponding to the limit of detection, x_{LOD}, was calculated. According to the Langmuir adsorption coefficient (K_{ads}) for DNA hybridization, a single monolayer has a value of 1.8×10^7 M^{-1}.[30] Equation 4 is used to convert the A_{30} ssDNA percentages into concentrations using the following relation:

$$c = \frac{\theta}{K_{ads}} \quad (4)$$

In eq 4, K_{ads} is 1.8×10^7 M^{-1} and θ is the percent coverage of A_{30} ssDNA. This corresponds to an x_{LOD} on shrunk PO-SiO_2 of 280 pM versus an x_{LOD} of 11 nM on glass. Hence, an overall 40-fold improvement in the LOD relative to a glass slide was noted.

For practical applications, fixing the probe concentration in order to determine the target concentration would likely be important. Therefore, we next fixed the % A_{30} ssDNA probe to 50% and decreased the target Cy3-DNA concentration to 1 μM, 0.1 μM, 0.05 μM, 0.01 μM, 0.005 μM, and 0.001 μM. We examined the amount of nonspecific binding by fixing the % A_{30} ssDNA probe to 0% and decreasing the target Cy3-DNA concentration in the same increments as mentioned. For each target concentration, we measured the fluorescence intensities from eight spots and repeated this three independent times. The LOD was calculated by taking 3 times the standard deviation of the background with 0.001 μM Cy3-DNA for the shrunk SiO_2 substrate and glass slide. The results for this experiment are presented in Figure 5. As apparent from the concentration curve (Figure 5), an approximate order of magnitude improvement in the LOD was observed on the shrunk PO-SiO_2 relative to the glass slide.

OUTLOOK

In this work, we have presented a rapid method to create DNA fluorescence microarrays using SiO_2 structures and demonstrated the ability to enhance the fluorescence signal of bound fluorophores. This demonstrates that the PO-SiO_2 substrate has higher detection sensitivity (280 pM) relative to planar glass surface (11 nM). Furthermore, a 30−45-fold improvement in the SNR was observed on the shrunk PO-SiO_2 substrate relative to a glass slide depending on the A_{30} ssDNA concentration. The fabrication of these substrates is simple, inexpensive, and can be readily integrated for microarray analysis. Furthermore, in contrast to MEF substrates, the enhanced fluorescence signals are uniform and not confined to nanometric hotspots. This ability to reach lower limits of detection could enable use of DNA microarrays for earlier disease diagnostics.

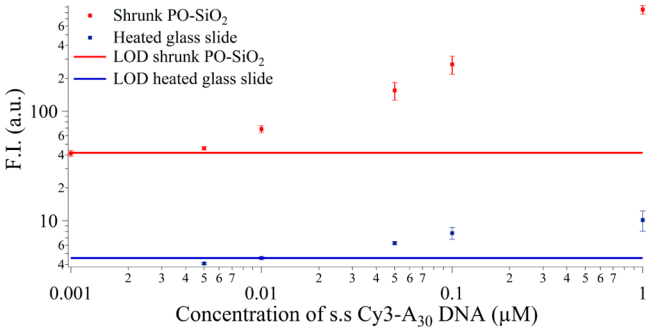

Figure 5. Summary of fluorescence intensities for DNA fluorescence microarray performed by changing the target Cy3 DNA concentration on shrunk PO-SiO_2 and heated glass slide with fixed 50% A_{30} ssDNA probe. The error bars are standard errors of mean.

ASSOCIATED CONTENT

Supporting Information

The unshrunk PO-SiO_2 results and confirmation of the chemical modification of the PO-SiO_2 substrates are available. This material is available free of charge via the Internet at http://pubs.acs.org.

AUTHOR INFORMATION

Corresponding Author

*E-mail: mkhine@uci.edu.

Author Contributions

‖H.S. and J.B.W. contributed equally to this work. The manuscript was written through contributions of all authors. All authors have given approval to the final version of the manuscript.

Notes

The authors declare no competing financial interest.

ACKNOWLEDGMENTS

This work is supported by the National Institute of Health (NIH) through the DP2 NIH Director's New Innovator Award (1 DP2 OD007283-01). R.M.C. and J.B.W. were supported by the NIH through grant R01-GM059622 on this work. SEM imaging was performed at the Laboratory for Electron and X-ray Instrumentation (LEXI) at UCI. The authors thank Dr. Nico Seefeld for her help with this paper.

REFERENCES

(1) Asanov, A.; Zepeda, A.; Vaca, L. A platform for combined DNA and protein microarrays based on total internal reflection fluorescence. *Sensors (Basel)* **2012**, *12* (2), 1800−15.

(2) Rhee, J. K.; Kim, K.; Chae, H.; Evans, J.; Yan, P.; Zhang, B. T.; Gray, J.; Spellman, P.; Huang, T. H.; Nephew, K. P.; Kim, S. Integrated analysis of genome-wide DNA methylation and gene expression profiles in molecular subtypes of breast cancer. *Nucleic Acids Res.* **2013**, *41* (18), 8464−74.

(3) Ma, L.; Su, M.; Li, T.; Wang, Z. Microarray-based fluorescence assay of endonuclease functionality and inhibition. *Analyst* **2013**, *138* (4), 1048−1052.
(4) Park, H. G.; Song, J. Y.; Park, K. H.; Kim, M. H. Fluorescence-based assay formats and signal amplification strategies for DNA microarray analysis. *Chem. Eng. Sci.* **2006**, *61* (3), 954−965.
(5) Li, X.; He, Y.; Zhang, T.; Que, L. Aluminum oxide nanostructure-based substrates for fluorescence enhancement. *Opt. Express* **2012**, *20* (19), 21272−7.
(6) DeLouise, L. A.; Kou, P. M.; Miller, B. L. Cross-correlation of optical microcavity biosensor response with immobilized enzyme activity. Insights into biosensor sensitivity. *Anal. Chem.* **2005**, *77* (10), 3222−3230.
(7) Oillic, C.; Mur, P.; Blanquet, E.; Delapierre, G.; Vinet, F.; Billon, T. DNA microarrays on silicon nanostructures: Optimization of the multilayer stack for fluorescence detection. *Biosens. Bioelectron.* **2007**, *22* (9-10), 2086−2092.
(8) Murthy, B. R.; Ng, J. K. K.; Selamat, E. S.; Balasubramanian, N.; Liu, W. T. Silicon nanopillar substrates for enhancing signal intensity in DNA microarrays. *Biosens. Bioelectron.* **2008**, *24* (4), 723−728.
(9) Le Berre, V.; Trevisiol, E.; Dagkessamanskaia, A.; Sokol, S.; Caminade, A. M.; Majoral, J. P.; Meunier, B.; Francois, J. Dendrimeric coating of glass slides for sensitive DNA microarrays analysis. *Nucleic Acids Res.* **2003**, *31* (16), e88.
(10) Schlapak, R.; Pammer, P.; Armitage, D.; Zhu, R.; Hinterdorfer, P.; Vaupel, M.; Fruhwirth, T.; Howorka, S. Glass surfaces grafted with high-density poly(ethylene glycol) as substrates for DNA oligonucleotide microarrays. *Langmuir* **2006**, *22* (1), 277−85.
(11) Kim, J. S.; Cho, J. B.; Park, B. G.; Lee, W.; Lee, K. B.; Oh, M.-K. Size-controllable quartz nanostructure for signal enhancement of DNA chip. *Biosens. Bioelectron.* **2011**, *26* (5), 2085−2089.
(12) Tsougeni, K.; Koukouvinos, G.; Petrou, P. S.; Tserepi, A.; Kakabakos, S. E.; Gogolides, E. High-capacity and high-intensity DNA microarray spots using oxygen-plasma nanotextured polystyrene slides. *Anal. Bioanal. Chem.* **2012**, *403* (9), 2757−2764.
(13) Wong, I. Y.; Melosh, N. A. An electrostatic model for DNA surface hybridization. *Biophys. J.* **2010**, *98* (12), 2954−63.
(14) Sabanayagam, C. R.; Lakowicz, J. R. Increasing the sensitivity of DNA microarrays by metal-enhanced fluorescence using surface-bound silver nanoparticles. *Nucleic Acids Res.* **2007**, *35* (2), e13.
(15) Malicka, J.; Gryczynski, I.; Lakowicz, J. R. DNA hybridization assays using metal-enhanced fluorescence. *Biochem. Biophys. Res. Commun.* **2003**, *306* (1), 213−218.
(16) Dragan, A. I.; Golberg, K.; Elbaz, A.; Marks, R.; Zhang, Y. X.; Geddes, C. D. Two-color, 30 second microwave-accelerated metal-enhanced fluorescence DNA assays: A new rapid catch and signal (RCS) technology. *J. Immunol. Methods* **2011**, *366* (1-2), 1−7.
(17) Qiang, W. B.; Li, H.; Xu, D. K. Metal enhanced fluorescent biosensing assays for DNA through the coupling of silver nanoparticles. *Anal. Methods-U.K.* **2013**, *5* (3), 629−635.
(18) Bras, M.; Dugas, V.; Bessueille, F.; Cloarec, J. P.; Martin, J. R.; Cabrera, M.; Chauvet, J. P.; Souteyrand, E.; Garrigues, M. Optimisation of a silicon/silicon dioxide substrate for a fluorescence DNA microarray. *Biosens. Bioelectron.* **2004**, *20* (4), 797−806.
(19) Oillic, C.; Mur, P.; Blanquet, E.; Delapierre, G.; Vinet, F.; Billon, T. Silicon nanostructures for DNA biochip applications. *Mater. Sci. Eng., C* **2007**, *27* (5-8), 1500−1503.
(20) Marino, V.; Galati, C.; Arnone, C. Optimization of fluorescence enhancement for silicon-based microarrays. *J. Biomed. Opt.* **2008**, *13* (5), 054060.
(21) Tarn, D.; Ashley, C. E.; Xue, M.; Carnes, E. C.; Zink, J. I.; Brinker, C. J. Mesoporous silica nanoparticle nanocarriers: Biofunctionality and biocompatibility. *Acc. Chem. Res.* **2013**, *46* (3), 792−801.
(22) Liang, S.; Shephard, K.; Pierce, D. T.; Zhao, J. X. Effects of a nanoscale silica matrix on the fluorescence quantum yield of encapsulated dye molecules. *Nanoscale* **2013**, *5* (19), 9365−73.
(23) Miletto, I.; Gilardino, A.; Zamburlin, P.; Dalmazzo, S.; Lovisolo, D.; Caputo, G.; Viscardi, G.; Martra, G. Highly bright and photostable cyanine dye-doped silica nanoparticles for optical imaging: Photophysical characterization and cell tests. *Dyes Pigm.* **2010**, *84* (1), 121−127.
(24) Pedone, A.; Prampolini, G.; Monti, S.; Barone, V. Realistic modeling of fluorescent dye-doped silica nanoparticles: A step toward the understanding of their enhanced photophysical properties. *Chem. Mater.* **2011**, *23* (22), 5016−5023.
(25) Titos-Padilla, S.; Colacio, E.; Pope, S. J. A.; Delgado, J. J.; Melgosa, M.; Herrera, J. M. Photophysical properties of $[Ir(tpy)_2]^{3+}$-doped silica nanoparticles and synthesis of a colour-tunable material based on an Ir(core)−Eu(shell) derivative. *J. Mater. Chem. C* **2013**, *1* (24), 3808−3815.
(26) Lin, S.; Sharma, H.; Khine, M. Shrink-induced silica structures for far-field fluorescence enhancements. *Adv. Opt Mater.* **2013**, *1* (8), 568−572.
(27) Commission on Spectrochemical and Other Optical Procedures for Analysis. Nomenclature, symbols, units and their usage in spectrochemical analysis. III. Analytical flame spectroscopy and associated non-flame procedures. *Spectrochim. Acta B* **1978**, *33* (6), 247−269.
(28) He, Z. L.; Zhou, J. Z. Empirical evaluation of a new method for calculating signal-to-noise ratio for microarray data analysis. *Appl. Environ. Microb.* **2008**, *74* (10), 2957−2966.
(29) Lee, J. S.; Song, J. J.; Deaton, R.; Kim, J.-W. Assessing the detection capacity of microarrays as bio/nanosensing platforms. *BioMed Res. Int.* **2013**, *2013*, 310461.
(30) Chen, Y.; Nguyen, A.; Niu, L.; Corn, R. M. Fabrication of DNA microarrays with poly(L-glutamic acid) monolayers on gold substrates for SPR imaging measurements. *Langmuir* **2009**, *25* (9), 5054−60.